Pure Appl. Chem., Vol. 78, No. 6, pp. 1173–1185, 2006.
doi:10.1351/pac200678061173

Reduction of perfluorinated compound emissions using atmospheric pressure microwave plasmas: Mechanisms and energy efficiency*

M. Nantel-Valiquette[1], Y. Kabouzi[1,‡], E. Castaños-Martinez[1], K. Makasheva[1], M. Moisan[1,†], and J. C. Rostaing[2]

[1]Groupe de Physique des Plasmas, Université de Montréal, Montréal H3C 3J7, Québec, Canada; [2]Air Liquide, Recherche et Dévelopement, 78354 Les Loges-en-Josas, France

Abstract: The abatement of perfluorinated compound (PFC) gases is investigated using atmospheric pressure microwave-surface-wave plasmas. These PFCs are diluted in nitrogen gas with concentration ranging from 5000 to 10 000 ppmv. The abatement mechanisms of SF_6 and CF_4 are examined, and conversion schemes are presented in the case where oxygen is added to the gas mixture. The PFC fragments are oxidized, forming acid-like by-products that are finally trapped irreversibly using a humidified soda lime scrubber. Gas-phase analysis was performed using Fourier transform infrared (FTIR) spectroscopy. The abatement efficiency is found to increase with increasing absorbed microwave power and gas residence time. The energy efficiency of the abatement process is shown to increase, with PFC concentrations in the gas mixture up to 10 000 ppmv. A complete conversion of SF_6 is achieved for energy densities ranging from 700 to 1200 J/cm^3 for concentrations ranging from 5000 to 10 000 ppmv. Lowering the microwave excitation frequency and using swirling flow are shown to reduce the energy cost per abated molecule.

Keywords: abatement of perfluorinated compounds; greenhouse gases remediation; plasmas; atmospheric pressure plasmas; microwave-surface-wave discharges.

INTRODUCTION

Perfluorinated compounds (PFCs), such as CF_4 and SF_6, have been identified, a decade ago, as highly potent global warming gases [1]. In addition to their strong infrared absorption cross-sections, PFCs have long atmospheric lifetimes. For instance, one metric ton of SF_6 is equivalent to 23 900 metric tons of CO_2, used as a reference gas, in terms of its potential effect on global warming over a 100-year time scale. Moreover, the estimated atmospheric lifetime for SF_6 is of the order of 3200 years, while that of CF_4 is 50 000 years. In the long term, PFC emissions into the atmosphere will make a major contribution to global warming trends and related climate changes. Despite these environmental concerns, PFCs are increasingly utilized in integrated-circuit manufacturing such as in dielectric-etch tools and plasma-enhanced chemical vapor deposition (PECVD) chamber cleaning. Reducing PFC emissions to comply

*Paper presented at the 17th International Symposium on Plasma Chemistry (ISPC 17), Toronto, Ontario, Canada, 7–12 August 2005. Other presentations are published in this issue, pp. 1093–1298.
‡Corresponding author: E-mail: yassine.kabouzi@umontreal.ca
†E-mail: michel.moisan@umontreal.ca

with voluntary or regulatory greenhouse emissions reduction roadmaps is still an important challenge for the semiconductor industry since these trends are expected to continue for the years to come.

Recently, several strategies have been considered by the semiconductor industry to reduce PFC emissions. For instance, remote NF_3 plasma sources (RPC) have been successfully implemented for cleaning PECVD chambers and are gaining wide acceptance in semiconductor manufacturing facilities [2]. RPC has very little residual PFC emissions because NF_3 is almost fully dissociated. Reduction of PFC emissions from etch tools for circuit patterns definition are achieved, in many cases, through plasma abatement devices at the exhaust level. This solution can be put into operation either at low or high pressure. At low pressure, the plasma abatement device is implemented in the tool foreline (pre-pump solution), where an undiluted PFC stream can be directly converted [3–12]. At high pressure, the plasma abatement device is implemented after the primary backing pump (post-pump solution), where the treated PFCs are diluted in nitrogen due to pump ballasting [13–19]. In both cases, high abatement efficiencies at relatively low energy consumption were reported [3–19].

The abatement method described in this article relies on microwave-surface-wave discharges operated at atmospheric pressure in nitrogen, as required for a post-pump solution. Oxygen is added to ensure oxidation of the PFC fragments. In this way, PFC fragments are transformed into thermodynamically stable acid-like fluorinated by-products. A humidified soda lime bed is utilized for irreversibly scrubbing the PFC converted by-products. Remediation of both SF_6 and CF_4 gases is examined for concentrations ranging from 5000 to 10 000 ppmv. Two strategies, involving lowering the microwave frequency and using gas swirling, are investigated and applied to the present plasma abatement system to reduce the energy cost per abated molecule.

The intent of the present article is to gain further insight into the abatement mechanisms and the energy efficiency of such an atmospheric pressure plasma solution, which is already in industrial use at several semiconductor factories.

CONSIDERATIONS ON PFC REACTION KINETICS IN ATMOSPHERIC PRESSURE MICROWAVE-SUSTAINED PLASMAS

All plasma-based abatement techniques have in common to provide electrons, free radicals, atoms, and molecules that initiate gas-phase reactions leading to the conversion of the pollutant molecule. Unlike the conversion of volatile organic compounds (VOCs) or nitrogen oxides (NO_x), where these pollutants can directly react with free radicals in the discharge, PFC molecules rarely react with radical species. This is due to the high chemical inertness and thermal stability of PFC molecules. Therefore, the initial rate-limiting reaction for the abatement of any PFC molecule is its dissociation through inelastic collisions with electrons. This initial electron-impact dissociation is followed by relatively fast atom-radical and radical-radical reactions, leading to the elimination of the pollutant molecule. Indeed, SF_x and CF_x fragments are known to have high reactivity with O, H, and OH radicals, on the same order of magnitude or slightly higher than with fluorine atoms [20]. PFC fragments can also react with each other, leading to the reformation of the PFC molecule. For instance, CF_3 can recombine either with F atoms, giving back CF_4 or with CF_3 to form C_2F_6. Although negligible at low pressure [10], reformation can be very important at high pressure (due to three-body reactions), thereby setting an upper limit on PFC abatement efficiency in atmospheric pressure plasmas.

Tables 1 and 2 present a selected set of kinetic reactions for the conversion of CF_4 and SF_6 when O_2 is added to the gas mixture, including electron-impact dissociation and neutral gas-phase reactions. The rate coefficients for neutral gas-phase reactions reported in Tables 1 and 2 have been taken from the literature [20–27]. These are given here for comparison purposes only since the values of rate coefficients listed for three-body reactions (RI-6 and RI-11, RII-12, RII-17 to 19, and RII-21) actually depend on gas pressure and therefore could differ from those applying to our experimental conditions (e.g., PFC partial pressure in the gas mixture).

Table 1 Electron-impact and gas-phase reactions for atmospheric pressure CF_4/O_2 plasmas. E is the threshold energy in eV unit and k the estimated rate coefficient in cm^3/s.

Electron-impact reactions	E (eV)	Gas-phase reactions	k (cm^3/s)
Neutral dissociation		I-6. $CF_3 + F \rightarrow CF_4$	2.01×10^{-11}
I-1. $e + CF_4 \rightarrow CF_3 + F + e$	12.5	I-7. $CF_3 + O \rightarrow COF_2 + F$	3.32×10^{-11}
I-2. $e + CF_4 \rightarrow CF_2 + 2F + e$	15.0	I-8. $CF_2 + O \rightarrow COF + F$	4.07×10^{-11}
I-3. $e + CF_4 \rightarrow CF + 3F + e$	20.0	I-9. $CF_2 + O \rightarrow CO + 2F$	4.00×10^{-12}
Dissociative attachment		I-10. $COF + O \rightarrow CO_2 + F$	9.30×10^{-11}
I-4. $e + CF_4 \rightarrow CF_3 + F^-$	4.8	I-11. $COF + F \rightarrow COF_2$	8.00×10^{-13}
I-5. $e + CF_3 \rightarrow CF_2 + F^-$			

Table 2 Electron-impact and gas-phase reactions for atmospheric pressure SF_6/O_2 plasmas. E is the threshold energy in eV unit and k the estimated rate coefficient in cm^3/s.

Electron-impact reactions	E (eV)	Gas-phase reactions	k (cm^3/s)
Neutral dissociation		II-12. $SF_5 + F \rightarrow SF_6$	1.66×10^{-11}
II-1. $e + SF_6 \rightarrow SF_5 + F + e$	9.6	II-13. $SF_4 + F \rightarrow SF_5$	1.30×10^{-11}
II-2. $e + SF_6 \rightarrow SF_4 + 2F + e$	12.1	II-14. $SF_5 + O \rightarrow SOF_4 + F$	2.10×10^{-11}
II-3. $e + SF_6 \rightarrow SF_3 + 3F + e$	16.2	II-15. $SF_3 + O \rightarrow SOF_2 + F$	2.00×10^{-11}
II-4. $e + SF_6 \rightarrow SF_2 + 4F + e$	18.6	II-16. $SF_2 + O \rightarrow SOF + F$	1.10×10^{-10}
II-5. $e + SF_6 \rightarrow SF + 5F + e$	22.7	II-17. $SOF + F \rightarrow SOF_2$	1.00×10^{-13}
Dissociative attachment		II-18. $SOF + O \rightarrow SO_2F$	1.00×10^{-10}
II-6. $e + SF_6 \rightarrow SF_5^- + F$		II-19. $SO_2F + F \rightarrow SO_2F_2$	5.00×10^{-11}
II-7. $e + SF_5 \rightarrow SF_4^- + F$	0.1	II-20. $SOF_3 + O \rightarrow SO_2F_2 + F$	5.00×10^{-11}
II-8. $e + SF_4 \rightarrow SF_3^- + F$		II-21. $SOF_3 + F \rightarrow SOF_4$	5.00×10^{-11}
II-9. $e + SF_4 \rightarrow SF_3 + F^-$	0.7		
Attachment–detachment			
II-10. $e + SF_6 \rightarrow SF_6^-$	0.2		
II-11. $SF_6^- \rightarrow SF_6 + e$			

At atmospheric pressure, CF_4 dissociation results from electron collisions and occurs most likely through dissociative attachment (RI-4) rather than dissociation into neutral fragments (RI-1 to 3). This is mainly due to a low electron average energy (≈1 eV), a characteristic of microwave discharges at atmospheric pressure. Then, CF_x radicals react with oxygen atoms to form COF_2, CO, and CO_2 as final and stable by-products. Reformation of CF_4 through RI-6 may also account for the particularly low conversion rate of CF_4 at atmospheric pressure.

The conversion pathway for SF_6 is more complicated than that for CF_4. In fact, the branching ratio of the SF_6 dissociation into neutral fragments has not been determined experimentally, though the study of Ito et al. [28] indicates that SF_2 accounts for most of the dissociation products of SF_6 followed by SF_3 and SF [27]. At atmospheric pressure, the dissociation of SF_6 into neutral fragments through electron impact (RII-1–5) is unlikely. For instance, considering a value of T_e of 1 eV, the rate coefficient for the total dissociation of SF_6 into neutrals ($\approx 2 \times 10^{-14}$ cm^3/s) is five orders of magnitude lower than the rate coefficient for dissociative attachment ($\approx 2.6 \times 10^{-9}$ cm^3/s for RII-6) due to a high energy threshold for SF_6 dissociation into neutrals. In contrast, in low-pressure plasmas where T_e is higher ($T_e \approx 3$ eV), the rate coefficient for dissociation into neutrals is 7.3×10^{-10} cm^3/s, close to the rate coefficient for dissociative attachment, which is 6.7×10^{-10} cm^3/s. Under the present atmospheric pressure conditions, the production of SF_x neutral fragments is more likely to proceed through electron attachment (RII-10) and dissociative attachment (RII-6 and RII-9) followed by charge-transfer reactions or mutual recombination with nitrogen positive ions. In SF_6/O_2 plasmas, all SF_x fragments, except SF_4,

react rapidly with oxygen atoms to form stable by-products such as SOF_4, SOF_2, and SO_2F_2 (see Table 2). Conversion pathways of CF_4 and SF_6 will be further discussed below.

RESULTS AND DISCUSSION

Fourier transform infrared (FTIR) spectroscopy has been employed for the identification of PFC by-products and the quantification of the abatement efficiency. This technique is easy to implement and provides reliable measurements whenever IR calibration standards are available. The destruction and removal efficiency (DRE) has been recorded as functions of discharge operating conditions, namely, absorbed microwave power, total flow rate, and PFC concentration. In all the experiments presented here, oxygen has been added to the gas mixture to ensure oxidation of PFC fragments. The addition of water vapor has also been tested and showed comparable, though slightly better, results than with oxygen. The DRE is defined as:

$$\mathrm{DRE}(\%) = \frac{[\mathrm{PFC}]_{\mathrm{in}} - [\mathrm{PFC}]_{\mathrm{out}}}{[\mathrm{PFC}]_{\mathrm{in}}} \times 100 \tag{1}$$

Detailed description of the experimental arrangement can be found in ref. [15]. Unless otherwise specified, the microwave excitation frequency was set to 2450 MHz.

Influence of the discharge operating conditions

Figure 1a shows the DRE for both SF_6 and CF_4 as a function of the absorbed microwave power, under a nitrogen flow rate of 30 standard liters per minute* (slm) containing 5000 ppm PFC in volume. The concentration of oxygen is set at 1.5 times the concentration of SF_6 or CF_4. Figure 1a shows that the DRE increases with increasing microwave power for both gases, the SF_6 abatement rate being, however, higher than that of CF_4 for the same absorbed microwave power level (P). For instance, at P = 3 kW the DRE amounts to 95 % with SF_6, while it is less than 55 % with CF_4. The observed increase of the DRE with power is due to the increase of both electron density and gas residence time. In surface-wave sustained discharges (SWDs), the plasma column length and the electron density are both proportional to the absorbed microwave power [29,30]. Increasing the electron density will obviously increase the dissociation rate of PFC molecules, thus resulting in a higher abatement efficiency. The influence of the residence time on the abatement efficiency is further shown in Fig. 1b, where the SF_6 DRE has been recorded as a function of the nitrogen flow rate. The SF_6 flow rate was kept constant at 203 standard cubic centimeters per minute (sccm). Figure 1b clearly shows that the DRE decreases linearly with increasing N_2 flow rate, regardless of the absorbed microwave power level. A higher N_2 flow rate results in a shorter gas residence time (on the average) in the plasma column, therefore, leading to a less and less complete dissociation of PFC molecules. A more accurate approach than simply that of residence time requires considering the influence of transport phenomena (diffusion and convection transport) on the abatement process.

*The gas flow rate is measured at room temperature and atmospheric pressure.

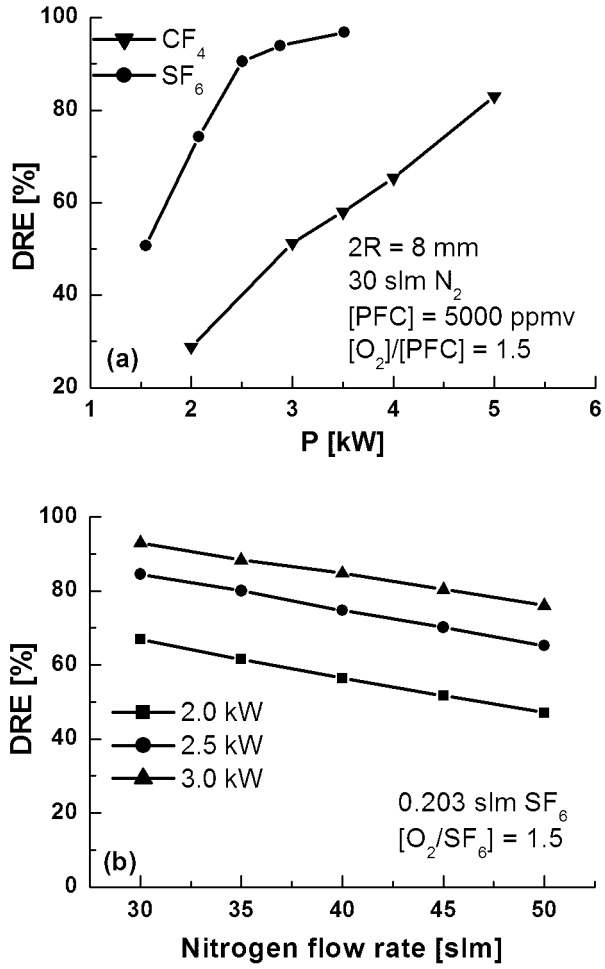

Fig. 1 (a) Observed DRE as a function of microwave power for SF_6 and CF_4 in a N_2/O_2 gas mixture, (b) observed SF_6 DRE as a function of N_2 flow rate, for three microwave power levels.

By-products analysis and PFC conversion schemes

Figures 2a and 2b present IR-spectra recorded at the exit of the discharge tube (before the soda lime scrubber) when abating CF_4 and SF_6, respectively, in a N_2/O_2 gas mixture. Past the scrubber, no hazardous acid-like by-products are left [15]. We notice from both spectra that no NO_x are detected, indicating a selective plasma chemistry in contrast to thermodynamic conditions.

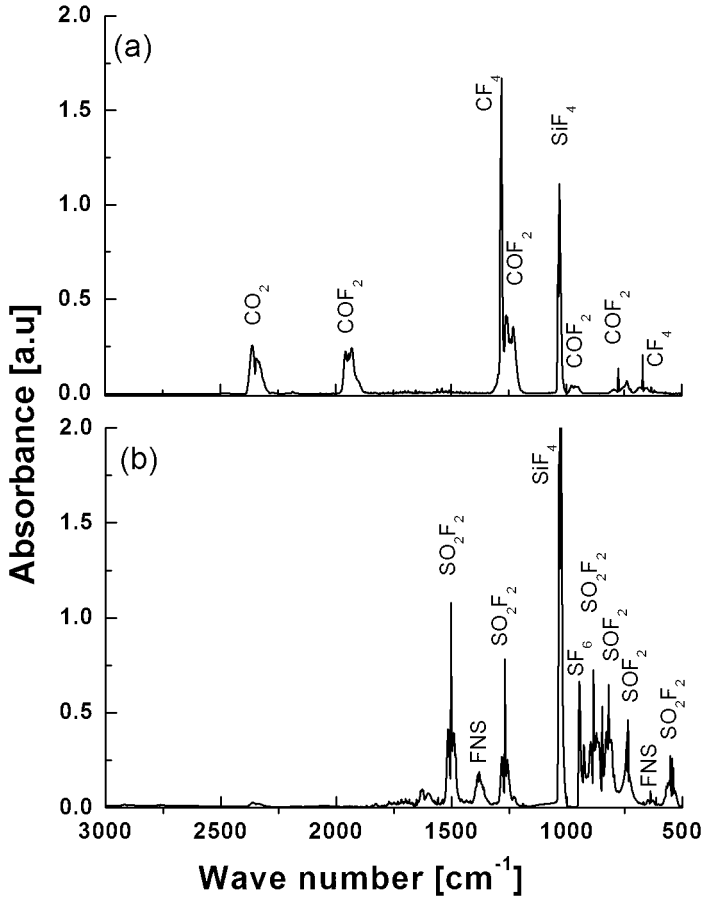

Fig. 2 IR spectra as observed after the plasma reactor (before the scrubber) for the abatement of (a) CF_4 and (b) SF_6, in N_2/O_2 gas mixture.

The CF_4 by-products in this N_2/O_2 atmospheric pressure plasma are mainly COF_2 and CO_2 as shown in Fig. 2a. Figure 3 summarizes the CF_4 conversion pathways. As discussed above, CF_3 is mainly produced here through dissociative attachment instead of direct dissociation into neutrals, as it is the case in low-pressure plasmas [10,21,22].

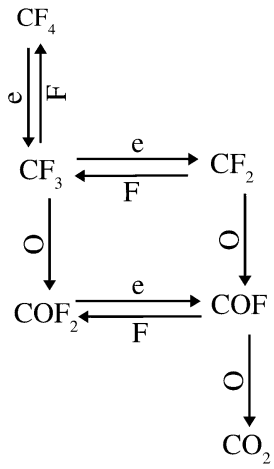

Fig. 3 Proposed CF_4 conversion pathways in atmospheric pressure microwave plasmas. Note that COF_2 and CO_2 are the final by-products at the plasma exhaust.

The observed by-products of the conversion of SF_6 at atmospheric pressure are: SOF_2, SO_2F_2, and FNS (see Fig. 2b). Although not detected in the IR-spectrum (no data available in the literature), SOF_4 has been detected by mass spectrometry [16] and is expected to be one of the main SF_6 by-products under our experimental conditions. Analysis of the IR-spectrum shows that SO_2F_2 is actually the dominant by-product. To further show this, Fig. 4 presents SF_6 by-products IR-band intensities as functions of the O_2 to SF_6 concentration ratio. We observe that the band intensity corresponding to SO_2F_2 increases with the $[O_2]/[SF_6]$ ratio, then reaches a plateau for a ratio higher than approximately 1.5. The band intensity corresponding to SF_6 shows the inverse trends (since DRE increases) when increasing the $[O_2]/[SF_6]$ ratio, reaching a plateau when this ratio exceeds unity. This is in accordance with previously reported results on DRE [15]. In contrast, the band intensities corresponding to SOF_2 and FNS go through a maximum at $[O_2]/[SF_6]$ equal to 0.7, before decreasing as oxygen concentration increases in the gas mixture.

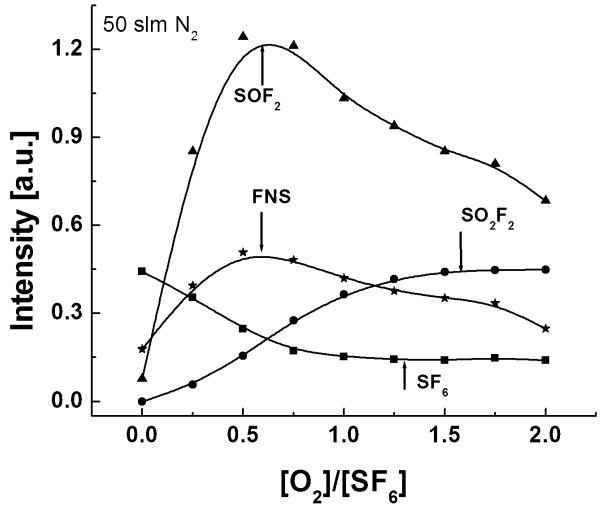

Fig. 4 SF_6 IR-band intensities as functions of the $[O_2]/[SF_6]$ ratio.

Figure 5 shows a possible conversion scheme for SF_6 at atmospheric pressure based on the observed stable SF_6 by-products and the arguments discussed above. The decomposition of SF_6 is assumed to occur through dissociative attachment, leading to SF_3 as the main precursor for the formation of SO_xF_y by-products. The conversion pathways shown in Fig. 5 consider SOF_2 as an intermediate product of SF_6 dissociation that leads to SO_2F_2 (and possibly to SOF_4) when oxygen is in excess in the gas mixture, in accordance with the experimental observations. The two main end-products are SOF_4 and SO_2F_2 (Fig. 4).

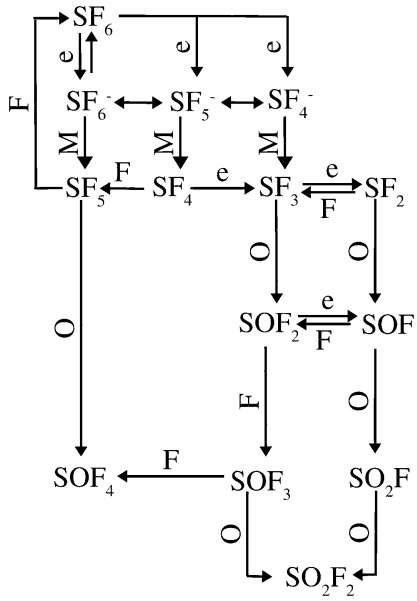

Fig. 5 Proposed SF_6 conversion pathways in atmospheric pressure microwave plasmas. Note that SO_2F_2 and SOF_4 are the final by-products at the plasma exhaust.

Process efficiency and scaling-law

Although convenient to employ, the DRE value is nonetheless only a relative measure of the degree of pollutant removal, since it depends on the amount of PFC gas entering the plasma reactor. The DRE concept has been utilized throughout most studies on PFC abatement. From the energy-efficiency point of view, it is preferable to record the amount of pollutant removed from or remaining in the gas stream as a function of the energy density absorbed in the plasma rather than the DRE value [31]. To see this, consider for instance a process that converts 80 % of 500 sccm of SF_6 and another that converts 95 % of 100 sccm of SF_6, both of them consuming the same level of power. Although the DRE is higher in the latter process, it is obvious that the process converting 80 % of 500 sccm of SF_6 is more energy-efficient. It is also worth noticing that it is the absolute PFC emission reduction (or its absolute residual level), and not the DRE, that makes sense for the practical enforcement of environmental policies.

Figure 6 shows the remaining SF_6 flow rate (in sccm) as a function of the energy density (in kJ/cm^3), for three N_2 flow rates and at a fixed SF_6 concentration of 7500 ppmv. The energy density (also denoted specific energy) is defined as the total absorbed microwave power (J/s) divided by the inlet SF_6 flow rate (a volume per unit time). This representation of the abatement process is, therefore, explicitly independent of the gas residence time and reactor dimensions, which makes it very useful for comparing different abatement systems. Said differently, the gas residence time is eliminated in this way because the PFC to N_2 concentration ratio is kept constant with increasing nitrogen flow rate: N_2 and SF_6

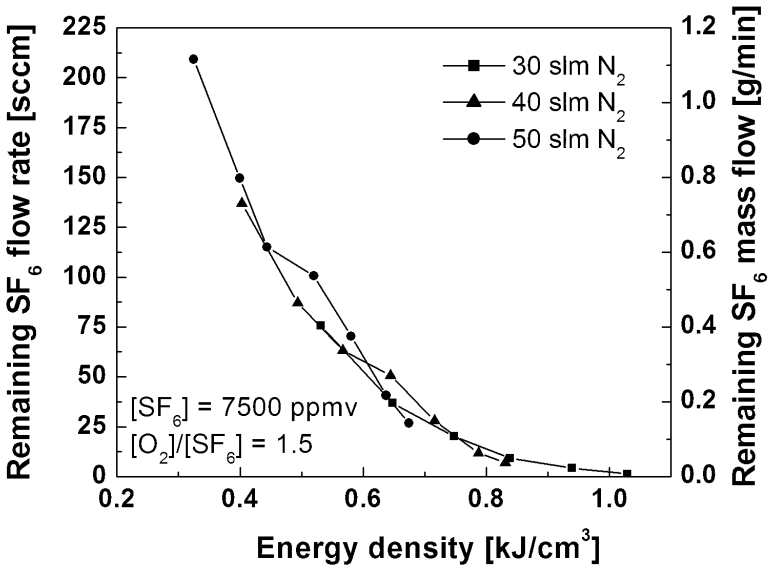

Fig. 6 Remaining SF_6 flow rate as a function of energy density, for three N_2 flow rates containing 7500 ppmv of SF_6.

mass flow rates therefore increase in the same proportion. We observe from Fig. 6 that, for a given SF_6 concentration, the remaining SF_6 flow rate is then only a function of the energy density: the abatement process obeys a scaling law. The energy cost for an almost complete conversion of SF_6 amounts to 1 kJ/cm^3 (or 233 eV per abated SF_6 molecule), under the present discharge operating conditions. The same trends have been obtained with CF_4 (not shown).

The energy density in Fig. 6, as mentioned above, refers to the total power divided by the PFC flow rate and not to the total flow rate, as it is commonly used in air pollutant removal using nonthermal plasmas (corona, dielectric-barrier, and electron-beam discharges) [31,32]. Our method is justified by the fact that the energy required for the abatement of SF_6 is determined by the energy required for dissociating this molecule. In the case of NO_x reduction in air using nonthermal plasmas, the primary reaction is the dissociation of N_2 molecules, not that of NO_x [31]. Thus, determining the energy density requires taking into account the N_2 flow rate; however, since in practice NO_x are very diluted, then there is not much difference when considering the total gas flow instead of that of the carrier gas.

Figure 7 shows that the higher the PFC concentration, at least up to 10 000 ppmv, the more energy-efficient is the abatement of SF_6: The energy cost per abated molecule is 40 % lower at 10 000 ppmv PFC concentration than at 5000 ppmv. Assuming that increasing the concentration of SF_6 in the gas mixture has little influence on the electron density and electron temperature, a higher SF_6 concentration will increase the frequency of dissociative attachment ($\nu_{\text{diss-attch}}[s^{-1}] = N_{\text{PFC}}[cm^{-3}] \times k_{\text{diss-attch}}[cm^3/s]$), resulting in a higher abatement efficiency (in terms of energy cost per abated molecule).

The previous results can be used to show that high-density plasma sources, such as surface-wave discharges, are more suitable for PFC abatement at atmospheric pressure than burners. Consider, for instance, thermal conversion of PFCs using a combustion process. Since the conversion of PFCs is an endothermic reaction, any increase of the PFC load will diminish the internal energy of the system (lowering the gas temperature), resulting in a decrease of abatement efficiency. Given the fact that the energy of the electrical field in a nonequilibrium plasma is predominantly transferred to electrons, high-density plasmas source are less sensitive to the PFC load and are, therefore, more energy-efficient than thermal processes.

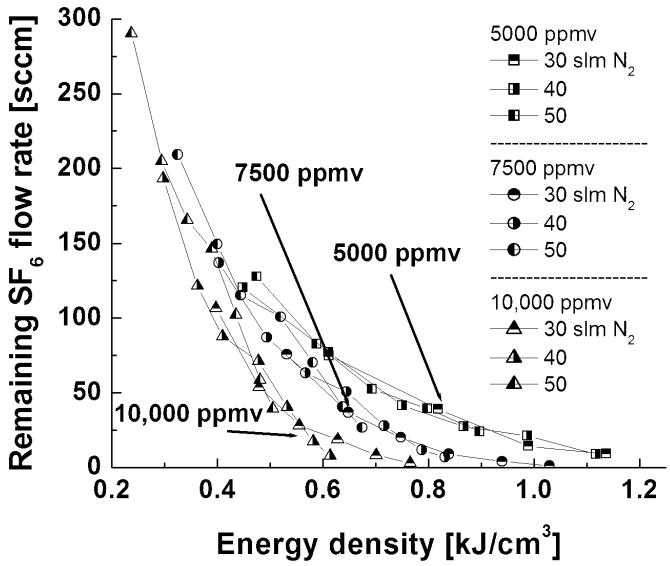

Fig. 7 Remaining SF_6 flow rate as a function of energy density, for three N_2 flow rates and three SF_6 concentrations in the gas mixture.

Strategies for improving the energy efficiency of the abatement process

We have tested two strategies to increase the energy efficiency of the surface-wave plasma abatement system.

The first one relies on increasing the plasma volume to increase the gas residence time. This was achieved by reducing the applied-field frequency: The plasma column length in SWDs increases when decreasing the field frequency because of a lower attenuation coefficient of the surface wave at lower frequencies [33]. Figure 8 shows the DRE as a function of the absorbed microwave power at two different field frequencies, namely, 915 and 2450 MHz. The nitrogen flow rate was fixed at 50 slm, and the SF_6 concentration was set to 5000 ppmv. We observe that a better abatement efficiency is achieved with the surface-wave discharge at 915 MHz: A 15 % DRE increase is obtained without additional energy cost. At a 90 % DRE (see Fig. 8), the power saving amounts to 1 kW when operating at 915 MHz.

The second strategy is to remedy the effect, on the abatement process, of the discharge contraction, which is characteristic of electrical discharges sustained at high pressure (>1.33 kPa) [29,30]. The plasma column of a contracted discharge is formed by a single filament, not filling entirely the discharge tube cross-section. In addition to contraction, high-frequency discharges can suffer filamentation, which is the breaking of a single plasma filament into several smaller filaments [29,30]. Radial contraction has been shown to greatly reduce the abatement efficiency of PFC gases in surface-wave discharges sustained at atmospheric pressure [15]. This is because the electron-free region between the plasma filament and the tube wall increases as the degree of contraction increases. A swirl-type flow [34] was used in this case to optimize the interaction between plasma electrons and PFC molecules in the discharge volume.

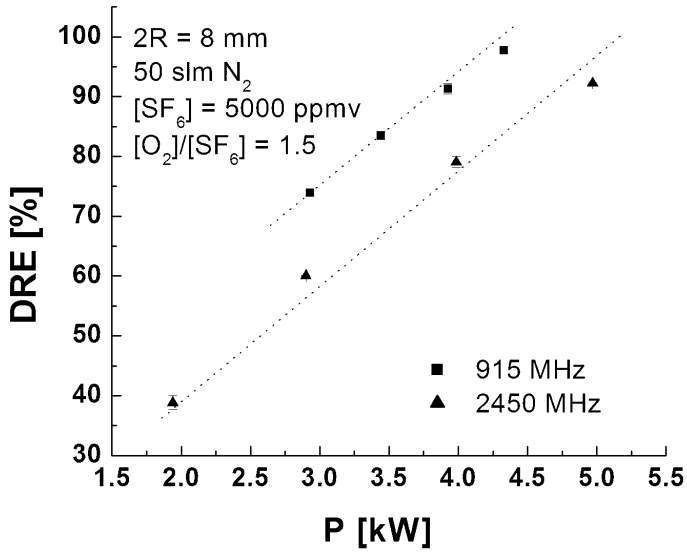

Fig. 8 Observed SF_6 DRE as a function of microwave power at two excitation frequencies.

Tangential gas injection has been used to ensure a swirling flow along the discharge tube. The gas-launchers have been designed and optimized to produce the swirling effect for gas flow rates ranging from 20 to 100 slm. Figure 9 shows the SF_6 DRE as a function of the absorbed microwave power, for a discharge with and without a swirling flow. The N_2 flow rate and the SF_6 concentration were kept constant at 50 slm and 5000 ppmv, respectively. We observe a net improvement of the abatement efficiency and a lowering of the energy consumption when a swirling flow is used. As shown in Fig. 9, a 24 % increase of the DRE is obtained with the swirling flow. Another way of looking at this energy-efficiency improvement is to consider a given DRE, say 90 % in Fig. 9, and observe that a 33 % power saving is then obtained. The energy cost per abated SF_6 molecule with the swirling flow is 177 eV/molecule, which is lower by 44 % than the energy cost without the swirling flow (300 eV/molecule, see Fig. 7).

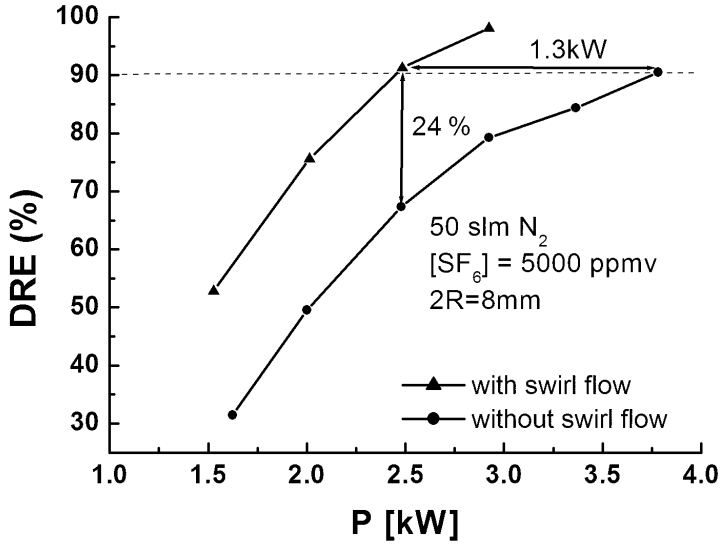

Fig. 9 Observed SF_6 DRE as a function of microwave power with and without swirling flow.

CONCLUSION

The abatement mechanisms of CF_4 and SF_6 in an atmospheric pressure N_2/O_2 microwave plasma have been identified. A conversion scheme for both gases has been proposed, based on the observed abatement by-products and on the estimation of the rate coefficient for several kinetic reactions. The energy efficiency of the present abatement system has been scrutinized. The abatement efficiency was shown to only depend on the energy density: the energy cost per abated PFC molecule. The energy cost per abated SF_6 molecule has been determined and was shown to decrease with increasing PFC concentration in the gas mixture (at least up to 10 000 ppmv). To lower the energy cost of the abatement process, two strategies were applied to the present system, namely, lowering the operating frequency and using a swirling flow. In the latter case, we were able to reduce by more than 40 % the energy cost per abated SF_6 molecule.

Finally, the insight gained into the abatement mechanisms of PFC gases shows how one could improve plasma-abatement schemes, in particular for the present and future needs of the semiconductor industry.

ACKNOWLEDGMENTS

The authors would like to thank A. El-Krid, C. Larquet, and D. Guérin for their valuable help with the experiments. The authors are also indebted to their technical staff: J.-S. Mayer, R. Lemay, R. Martel, M. Robert, T. Aral, and L. Goyet for their professional and constant support. Y. K. would like to thank Prof. D. B. Graves and C-C. Hsu (UC Berkeley) for their valuable comments and discussions on PFC abatement. This work was supported by the Centre de Recherche Claude-Delorme of the Groupe Air Liquide (France) and by Air Liquide Canada.

REFERENCES

1. <http://unfccc.int/resource>.
2. S. Raoux, T. Tanaka, M. Bhan, H. Ponnekanti, M. Seamons, T. Deacon, L.-Q. Xia, F. Pham, D. Silvetti, D. Cheung, K. Fairbairn. *J. Vac. Sci. Technol., B* **17**, 477 (1999).
3. R. Jewett. *Future Fab. Int.* **12**, 77 (2002).
4. C. L. Hartz, J. W. Bevan, M. W. Jackson, B. A. Wofford. *Environ. Sci. Technol.* **32**, 682 (1998).
5. B. A. Wofford, M. W. Jackson, C. Hartz, J. W. Bevan. *Environ. Sci. Technol.* **33**, 1892 (1999).
6. V. Mohindra, H. Chae, H. H. Sawin, M. T. Mocella. *IEEE Trans. Semicond. Manuf.* **10**, 399 (1997).
7. S. A. Vital, H. Sawin. *J. Vac. Sci. Technol., A* **18**, 2217 (2000).
8. E. Tonnis, D. Graves, V. Vartanian, R. Jewett, L. Beu, T. Lii. *J. Vac. Sci. Technol., A* **18**, 393 (2000).
9. A. Fiala, S. Mahnovski, M. W. Kiehlbauch, D. B. Graves. *J. Appl. Phys.* **86**, 152 (1999).
10. M. W. Kiehlbauch, D. B. Graves. *J. Appl. Phys.* **86**, 2047 (2001).
11. X. P. Xu, S. Rauf, M. J. Kushner. *J. Vac. Sci. Technol., A* **18**, 213 (2000).
12. M. Y. Liao, K. Wong, J. P. McVittie, K. Saraswat. *J. Vac. Sci. Technol., B* **17**, 2638 (1999).
13. S. J. Yu, B. Chang. *Plasma Chem. Plasma Process.* **21**, 311 (2001).
14. L. Fabian. *Future Fab. Int.* **12**, 61 (2002).
15. Y. Kabouzi, M. Moisan, J. C. Rostaing, C. Trassy, D. Guérin, D. Kéroack, Z. Zakrzewski. *J. Appl. Phys.* **93**, 9483 (2003).
16. J. C. Rostaing. *Future Fab. Int.* **14**, 55 (2003).
17. Y. C. Hong, H. S. Kim, H. Uhm. *Thin Solid Films* **435**, 329 (2003).
18. Y. Kim, K. T. Kim, M. S. Cha, Y.-H. Song, S. J. Kim. *IEEE Trans. Plasma Sci.* **33**, 1041 (2005).
19. M. Nagai, M. Hori, T. Goto. *J. Appl. Phys.* **97**, 123304 (2005).
20. R. J. Van Brunt, J. T. Herron. *IEEE Trans. Elec. Insul.* **25**, 75 (1990).
21. K. R. Ryan, I. C. Plumb. *Plasma Chem. Plasma Process.* **6**, 205 (1986).
22. K. R. Ryan, I. C. Plumb. *Plasma Chem. Plasma Process.* **6**, 231 (1986).
23. K. R. Ryan, I. C. Plumb. *Plasma Chem. Plasma Process.* **8**, 263 (1988).
24. K. R. Ryan, I. C. Plumb. *Plasma Chem. Plasma Process.* **10**, 207 (1990).
25. A. Picard, G. Turban, B. Crolleau. *J. Phys. D* **19**, 991 (1986).
26. L. G. Christophorou, K. Oltoff, M. V. V. S. Rao. *J. Phys. Chem. Ref. Data* **25**, 1341 (1996).
27. L. G. Christophorou, K. Oltoff. *J. Phys. Chem. Ref. Data* **29**, 267 (2002).
28. M. Ito, M. Goto, H. Toyoda, H. Sugai. *Contrib. Plasma Phys.* **35**, 405 (1995).
29. Y. Kabouzi, M. D. Calzada, M. Moisan, K. C. Tran, C. Trassy. *J. Appl. Phys.* **91**, 1008 (2002).
30. E. Castaños-Martinez, Y. Kabouzi, K. Makasheva, M. Moisan. *Phys. Rev. E* **70**, 066405 (2004).
31. B. M. Penetrante, J. N. Bradsley, M. C. Hsiao. *Jpn. J. Appl. Phys.* **36**, 5007 (1997).
32. L. A. Rosocha, R. A. Korzekwa. *J. Adv. Oxid. Technol.* **4**, 247 (1999).
33. M. Moisan, J. Pelletier. *Microwave Excited Plasmas*, Elsevier, New York (1992).
34. A. Gutsol, J. A. Bakken. *J. Phys. D* **31**, 704 (1998).